Simulating Alzheimer's by Calculating the Effects of Neuronal Death and Malfunction on Brain Frequency Bands

Minho Choi, Garrett Jones

December 10th, 2023

Abstract

In Alzheimer's disease, the power of different frequency bands as measured by EEG shifts as the disease progresses. Generally, the higher frequency bands (alpha, beta, gamma) decrease in power, while the lower frequency bands (delta, theta) increase in power. The paper by Abuhassan et. al. [1] presents two neural network models that simulate the effects of neural degeneration on the frequency band powers. In the present paper, one of the models, called the larger network model, is employed to test two hypotheses proposed in Abuhassan et. al [1]. The first hypothesis investigates the impacts of neuronal deaths on frequency band powers, and the second hypothesis examines the impacts of malfunctioning neuron sensitivity on frequency band powers. The results of the two hypotheses in Abuhassan et. al [1] are reproduced; in addition, a new hypothesis, testing the effects of malfunctioning post-spike recovery of neurons, is studied to see if it better replicates the band power shifts as measured by EEG compared to the first and second hypotheses. The new hypothesis is tested using the larger network model. Based on the results, the malfunctioning recovery decreases the higher frequency band powers less than the two hypotheses in Abuhassan et. al [1], while it increases the low frequency band powers more than them.

1 Introduction

Alzheimer's disease (AD) is a common neurodegenerative disorder with no known cure. There are many diagnostic tools used to diagnose AD, one of which is the electroencephalogram (EEG). Based on a literature survey, the accuracy of EEG in detecting AD is approximately 80% [5]. An EEG measures the firing of neurons in the brain. The results are analyzed by separating the data into standardized frequency bands: delta (up to 4 Hz), theta (4–8 Hz), alpha (8–13 Hz), and beta (13–25 Hz) [7].

In the EEG data of patients with AD, alpha and beta band powers are lower than for non-AD patients, while theta and delta band powers are higher [5]. Additionally, these shifts are more pronounced with the severity of AD [5]. If the shifts in beta band power observed in AD can be traced back to specific types of degradation in neurons, that would aid in our understanding of the disease, allowing us to target interventions more effectively.

In the paper by Abuhassan et. al. ([1]), the authors investigated the relationship between EEG band power changes and AD. They used two types of networks: 1) a conductance-based local neuronal network, and 2) a simple large network model. The local neuronal network contained 200 total neurons: 160 excitatory cells (e-cells) and 40 inhibitory cells (i-cells), and

the neurons used Hodgkin-Huxley dynamics. The authors focused on detecting a reduction in the beta power band in the local neuronal network. For the baseline of the simple large network model, it contained 1000 neurons, with 800 e-cells and 200 i-cells. They tried out two case studies on the large network model. In case study 1, they reduced the number of e-cells and compared to baseline, and in case study 2, they reduced the sensitivity of e-cells and compared to the baseline. The authors computed the impact on the power of each frequency band and found that the beta band was impacted the most.

Other papers have also investigated the effects of neuronal dysfunction on EEG power bands. Xin Zou et. al. created a model of the hippocampus with four types of neurons: excitatory pyramidal neurons, inhibitory basket interneurons, OLM interneurons, and inhibitory MSGABA interneurons, all of which have been demonstrated to enhance the theta power band in rats [8]. The authors showed with their model that only a decrease in a particular type of channel (fast-inactivating K^+ currents) had an effect on theta band power. In particular, the decreased currents led to increased excitability of pyramidal neurons, increasing theta band power.

Bhattacharya et. al. investigated the effect of disturbing neural cell populations in a thalamo-cortico-thalamic model [2]. This model incorporates a thalamic component containing thalamic relay cells, interneurons, and the thalamic reticular formation, and secondly a cortical component containing pyramidal cells, excitatory interneurons, slow inhibitory interneurons, and fast inhibitory interneurons. With their simulations, they showed that both reducing the total inhibitory cell population and reducing the synaptic count of inhibitory neurons resulted in a reduction of alpha band power.

Culmone et. al. modeled the smaller-scale impact of AD by building a model to test impact of the reduction of different types of conductances on the excitatory behavior of a single pyramidal neuron with 100 synapses [3]. The complication is that β-amyloid (Aβ) can either make a neuron more excitable with some effects (such as reducing K^+ currents) or make it less excitable with other effects (such as reducing NA^+ current). The authors found that including all effects together resulted in reduced excitability.

This collection of papers looks at a complementary collection of dynamics seen in AD neurons and neural networks. Our subject paper ([1]) looks at the impact on beta band power, Xin Zou et. al. ([8]) look at the impact on theta band power, and Bhattacharya et. al. ([2]) look at alpha band power. Lastly, Culmone et. al. ([3]) look at neuron excitability. A missing piece seems to be a model that can explain all of the observed frequency power band changes seen in AD, but we could not find a paper that attempted to do that. Therefore, in the present paper, we mainly focus on the decreases in high frequency band powers, especially in alpha and beta, and increases in low frequency band powers, such as delta and theta.

In **Section 2**, the details of the model for spiking neuron are discussed. Moreover, the setting of the simulations is specified, and the process of the power spectrum analysis is explained. In **Section 3**, the reproduction of the results for the two hypotheses in Abuhassan et. al. [1] are evaluated. In **Section 4**, the novel question is asked and answered. Lastly, the paper ends with the conclusion in **Section 5**. All references are included in **Section 6**, and all codes are included in **Section 7**.

2 Model Description

2.1 Spiking Neuron

The authors of [1] use the model of spiking neurons from [4]. The following two dimensional ordinary differential equations (ODEs) represent the model:

$$\begin{aligned} \frac{dV}{dt} &= 0.04V^2 + 5V + 140 - u + I \\ \frac{du}{dt} &= a(bV - u) \end{aligned} \tag{1}$$

After every spike, a neuron is reset with this rule:

$$\text{if } V \geq 30\ mV,\ \text{then } V \leftarrow c, u \leftarrow u + d$$

where the variable t represents time, the variable V represents membrane potential and u represents the recovery of a neuron. The plots of the ODEs are the following:

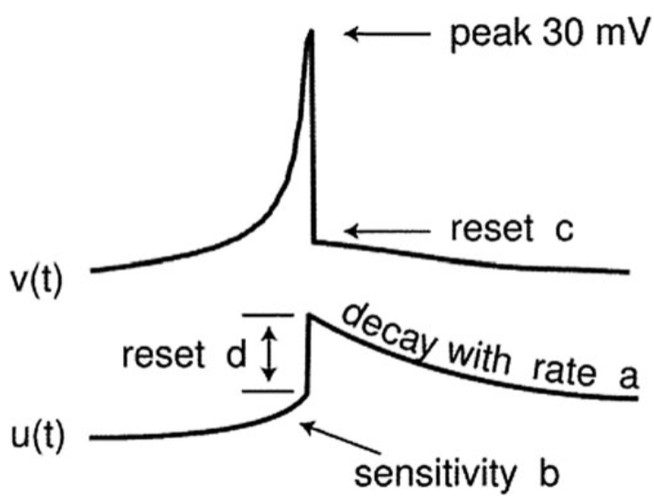

Figure 1: Plots of the ODEs in [4]

The variables and parameters can be understood more clearly when looking at the plots. There is a spike when the variable V reaches $+30\ mV$. After a spike, the value of V is reset to the value of parameter c. Next, the recovery variable u provides a negative feedback to the membrane potential variable V to simulate a neuron with recovery time. Due to the variable

u in the simulation, after a neuron spikes, it can not spike again right away. The recovery time is determined by the parameters a and d. First, the parameter a value represents a decay rate of u. Hence, a lower a value means that a neuron's recovery time becomes longer, resulting less frequent spiking of the neuron. Next, the parameter d value represents the after-spike reset of u. After a spike, the u variable is reset to $u + d$ so that the neuron does not reach the spiking threshold until u value decreases enough for next spike. Lastly, the parameter b represents how sensitive u is to changes in V. Hence, a lower b value couples the variables V and u more weakly, resulting in high-threshold spiking dynamics [4]. The values of the parameters depend on the type of a neuron, but typical values of the parameters are the following for a "regular spiking" neuron:

- $a = 0.02$
- $b = 0.2$
- $c = -65\ mV$
- $d = 2$

The variable I in the ODEs (1) represents either synaptic currents or dc-currents injected directly into a neuron [4]. Synaptic current is the input received from the spikes from other neurons in the network through simulated synapses, and the injected dc-currents are the input directly induced in the neuron. Thus, the variable I describes how neurons in a network are connected to each other and how they are affecting each other.

2.2 Simulation

To reproduce the computational model from [1], we acquired a Python translation of the MATLAB code provided in [4]. For the control (baseline) group, 1000 neurons are used, where 800 neurons are excitatory (e-cells) and 200 neurons are inhibitory (i-cells). The ratio of 4 to 1 between the e-cells and i-cells is motivated by the anatomy of the mammalian cortex [1]. All 1000 neurons are fully connected to each other with randomized synaptic weights. The values of parameters a, b, c and d for e-cells and i-cells are summarized in the following table, which is based on [4]:

Types	Number	a	b	c	d
e-cells	800	0.02	0.2	$-65 + 15r^2$	$8 - 6r^2$
i-cells	200	$0.02 + 0.08r$	$0.25 - 0.05r$	-65	2

Figure 2: Setting for Control Group

where r is a random variable selected from uniform distribution between 0 and 1, and is different for each neuron. For initial conditions, V is set to -65 and u is set to $b \times V$ for each neuron.

The simulation is run for 30,000 ms (30 seconds) with a time resolution of 1 ms. The first 29,000 ms is a settlement period for stability of the simulation, and power spectrum

analysis is applied to the last 1000 ms. The variables V and u are approximated using the Forward Euler method every 1 ms. The simulation of 30 seconds is repeated for 10 trials to obtain the mean power spectrum.

2.3 Power Spectrum

The following two example plots are useful to understand how the power spectrum is calculated using the values obtained from the simulation:

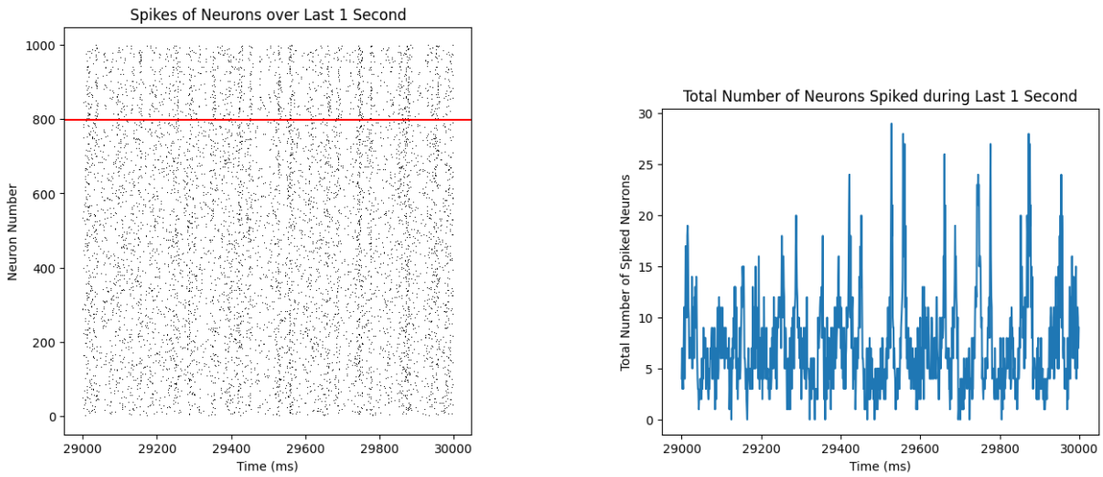

(a) Spikes of neurons over the last 1 Second

(b) Total number of spikes per 1 ms

Figure 3: Results Obtained After Simulation

Figure 3a shows the spikes of neurons over last 1 second, where the black dots represent the spikes. The dots below the red line in Figure 3a are the spikes of e-cells, while the dots above the red line are the spikes of i-cells. Figure 3b displays the total number of spikes per 1 ms. It is hard to see the power of each frequency band just by looking at the plots in Figure 3. Hence, the power spectrum analysis is performed using Welch's method [6]. The Welch's method employs Fast Fourier Transform to convert signal from time domain to frequency domain. As a result, the following plot is obtained:

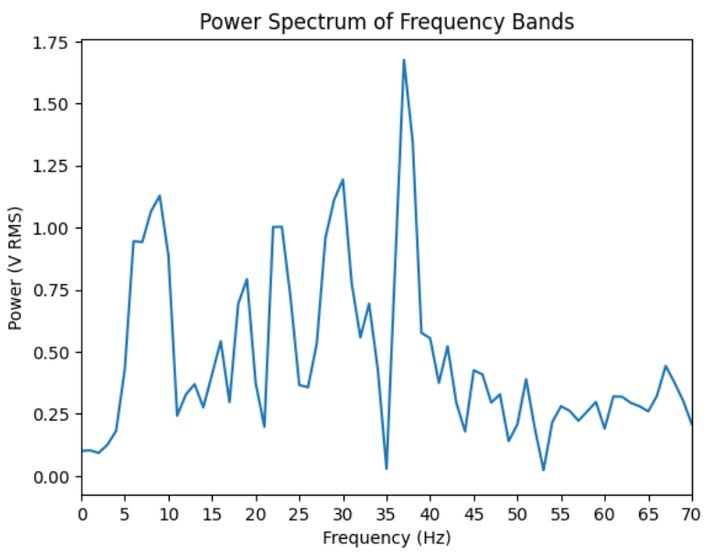

Figure 4: Power Spectrum of Frequencies

The last step is to apply the Riemann sum to calculate the power of each frequency band. For example, the power of theta frequency band is sum of power values between 4 Hz and 8 Hz. This same process of calculating the power spectrum is repeated for 10 trials. Consequently, the mean power spectrum is obtained from the 10 trials for the control group.

3 Reproduction

Two case studies are explored in Abuhassan et. al. [1]. The first case study investigates the effects of neuronal deaths on the frequency band powers. The second case study explores the effects of neuronal dysfunction on the frequency band powers. The specific parameter values of each case study are found in the corresponding subsection. For the reproduction, the frequency bands are divided into 8 categories: delta (1-3 Hz), theta (4–7 Hz), alpha (8–12 Hz), beta1 (13–18 Hz), beta2 (19–21 Hz), beta3 (22–30 Hz), gamma (31–50 Hz), and full (1-70 Hz), as in [1].

Before comparing the results from [1] and the reproduced values, there are several aspects to note. First, only the model for spiking neuron is explicitly stated in [1], so using the total number of spikes per 1 ms for the power spectrum analysis may be different to what the authors did in [1]. Next, there are various methods to perform the power spectrum analysis, such methods as Periodogram, Welch and Multitaper. Among different methods, Welch's method is employed to reproduce the results, while the authors in [1] may have used other methods to obtain the frequency band powers (which they did not specify in the paper). Lastly, there is significant randomness in the simulation. In Figure 2, the variable r is applied to many parameters. In addition, the variable I in the ODEs (1) consists of random variables. Therefore, there are discrepancies in the values between the results from [1] and the reproduction; however, the qualitative results are similar.

3.1 Case Study 1

For Case Study 1, the effects of neuronal deaths are examined by decreasing number of e-cells in the network. The settings of the parameters for this case study are summarized in the following table:

Types	Number	a	b	c	d
e-cells	**764–794**	0.02	0.2	$-65 + 15r^2$	$8 - 6r^2$
i-cells	200	$0.02 + 0.08r$	$0.25 - 0.05r$	-65	2

Figure 5: Setting for Case Study 1

The only difference with the control group is that the simulation is ran with fewer e-cells. The number of e-cells is decreased from 794 to 764 with a step size of 2. Hence, 16 different

numbers of e-cells are tested in total. For each number of e-cells, the simulation is repeated for 10 trials to obtain the mean power spectrum values. After all simulations are finished, the lowest mean power spectrum value is chosen for the comparison to the control group. The results from the paper and the reproduced values are summarized in the following table:

Frequency band	Min. value	Control value	Decrease percentage
Delta	3.498	3.737	6.4%
Theta	2.71	3.104	12.7%
Alpha	3.178	4.236	**25%**
Beta3	6.125	7.326	16.4%
Gamma	13.15	15.034	12.5%
Full	44.25	50.306	12%

(a) From Abuhassan et. al. [1]

Frequency band	Min. value	Control value	Decrease percentage
Delta	0.299	0.357	16.15%
Theta	1.503	1.705	11.81%
Alpha	2.515	3.657	**31.24%**
Beta1	2.237	2.891	22.65%
Beta2	1.263	1.429	11.62%
Beta3	4.687	5.756	18.57%
Gamma	9.133	10.738	14.94%
Full	26.733	31.548	15.26%

(b) Reproduction

Figure 6: Reproduction of Case Study 1

As previously mentioned, the values are not similar to each other. However, the largest percentage decrease occurs in the alpha frequency band in both tables. Moreover, in general, the percentage decreases of high frequency band powers (alpha, beta1, beta3) are greater than those of the low frequency band powers (delta, theta). Thus, the exact values cannot be reproduced, but the qualitative results, such as alpha frequency band power decreasing the most, were reproduced.

3.2 Case Study 2

For Case Study 2, the effects of neuronal dysfunction are examined by decreasing the parameter b value. The settings of the parameters for this case summary are summarized in the following table:

Types	Number	a	b	c	d
e-cells	800	0.02	**0.195–0.1995**	$-65 + 15r^2$	$8 - 6r^2$
i-cells	200	$0.02 + 0.08r$	$0.25 - 0.05r$	-65	2

Figure 7: Setting for Case Study 2

The only difference with the control group is that the simulation is run with a smaller parameter b value for e-cells. The parameter b value for e-cells is decreased from 0.1995 to 0.195 with a step size of 0.0005. Hence, 10 different parameter b values are tested in total. For each parameter b value, the simulation is repeated for 10 trials to obtain the mean power spectrum values. After all simulations are finished, the lowest mean power spectrum value is chosen for the comparison to the control group. The results from the paper and the reproduced values are summarized in the following table:

Frequency band	Min. value	Control value	Decrease percentage
Delta	3.208	3.737	14.2%
Theta	2.554	3.104	18%
Alpha	2.937	4.236	30.7%
Beta1	2.671	2.891	25.4%
Beta2	1.105	1.429	**38.7%**
Beta3	5.359	7.326	26.9%
Gamma	11.557	15.034	23.1%
Full	39.326	50.306	21.8%

(a) From Abuhassan et. al. [1]

Frequency band	Min. value	Control value	Decrease percentage
Delta	0.294	0.357	17.66%
Theta	1.752	1.705	-2.80%
Alpha	2.197	3.657	**39.93%**
Beta1	2.137	2.891	26.10%
Beta2	1.333	1.429	6.68%
Beta3	4.385	5.756	23.81%
Gamma	7.307	10.738	31.96%
Full	24.817	31.548	21.34%

(b) Reproduction

Figure 8: Case Study 2

There are several differences between the results from [1] and the reproduced values for Case Study 2. First, the largest percentage decrease happens in beta2 frequency band power in [1]. Conversely, the largest percentage decrease in our reproduction occurs in alpha frequency band power. Perhaps the most surprising difference is that in our reproduction, beta2 frequency band power had the lowest percentage decrease among the high frequency band powers, whereas in the original paper, this band had the largest decrease. This discrepancy might have occurred due to the randomness in the simulation or because of the power spectrum analysis methods chosen.

Comparing the impact on alpha frequency band power, this band had the highest percentage decrease in our reproduction of Case Study 2, while in [1], the alpha frequency band power's percentage decrease was the second largest. The large decrease in alpha frequency band power from both results matches the results from [2]. Comparing the impact on theta frequency band power, the results in [1] and our reproduction are in the opposite direction. However, our results match better with the model in [8] and the real EEG data in [5]. Thus, although there are discrepancies between the results from [1] and the reproduced values, the qualitative results of our reproduction more closely agrees with the computational models in [8] and [2] and real EEG data.

4 Novel Results

The simulation in [1] only focused on the reduction of beta band power, and did not attempt to replicate the changes seen in the power of other frequency bands for EEGs of AD patients. For our novel simulation, we decided to change a different parameter than the authors to see if the distribution of frequency band changes would match the changes seen in AD better. We chose to vary parameter a in the model. The setting of the novel question is summarized in the following table:

Types	Number	a	b	c	d
e-cells	800	**0.0195–0.01995**	0.2	$-65 + 15r^2$	$8 - 6r^2$
i-cells	200	$0.02 + 0.08r$	$0.25 - 0.05r$	-65	2

Figure 9: Setting for Novel Questions

The only difference with the control group is a smaller parameter a value for e-cells. The simulation is run with parameter a for e-cells set to values between 0.01995 and 0.0195, with a step size of 0.00005. Hence, 10 different parameter a values are tested in total. For each parameter a value, the simulation is repeated for 10 trials to obtain the mean power spectrum values. After all simulations are finished, the lowest mean power spectrum value is chosen for the comparison to the control group. The results of the simulation are summarized in the following table:

Frequency band	Min. value	Control value	Decrease percentage
Delta	0.285	0.357	**20.32%**
Theta	1.767	1.705	-3.65%
Alpha	3.009	3.657	17.72%
Beta1	2.378	2.891	17.75%
Beta2	1.377	1.429	3.66%
Beta3	5.038	5.756	12.46%
Gamma	9.795	10.738	8.78%
Full	29.685	31.548	5.91%

Figure 10: Decreasing parameter value a

This parameter modification performed worse overall than the two case studies from [1]. The largest decrease was in the delta frequency band power, whereas in EEG data, the delta band power increases. In this simulation, the decrease in the delta frequency band power was even larger than alpha, beta 1, beta 2, and beta 3, which was unexpected. Moreover, the decrease percentages in high frequency band powers are lower than the two case studies. However, the slight increase in the theta frequency band power does match EEG results, as mentioned in Bhattacharya et. al. ([2]). Thus, increasing recovery time of neurons have relatively less effect on the frequency band powers than the death of neurons and malfunction in the sensitivity of neurons.

5 Conclusion

The goal of Abuhassan et. al. ([1]) was to investigate how two different neural network models replicate abnormal power band shifts in neural network firing patterns of brains with AD. They used two different models - 1) a local neuronal network based on Hodgkin-Huxley dynamics, and 2) a simple large network model based on the model from Izhikevich ([4]).

For the second model, they performed two case studies, 1) simulating neuronal death by reducing excitatory neurons, and 2) simulating lower sensitivity of neurons by modifying the sensitivity parameter of the recovery variable. They ran their simulations multiple times and averaged the effects on the power bands. Their results showed that beta band power reduced the most.

We were able to replicate most of the qualitative results from Abuhassan et. al. ([1]), and where our replications differed, they actually matched the qualitative changes seen in EEG results of AD brains better. In particular, the results in [1] showed a decrease in theta band frequency power, whereas our replication showed an increase, which qualitatively matches EEG results. The results of our novel experiment, where we increased the recovery time of neurons to lengthen the time between spikes, were a worse fit for the qualitative changes seen in EEG, so we reject it as an explanation of neuronal changes in AD. Overall, we confirmed the general conclusion of [1], which was that the malfunction of excitatory neurons is a significant contributor to the lowering of the power of high frequency bands of EEG for AD patients.

The excitatory neurons and high frequency band powers are only part of the story, though. As noted in the introduction, both lower frequency bands (delta and theta) are increased in AD, not merely in a relative sense. Additionally, [2] showed that reducing the number of inhibitory neurons in certain circuits (in their case, a thalamo-cortico-thalamic model) decreases alpha band power. In order for a model to show the complete range of effects seen in EEG (increasing delta/theta, decreasing alpha/beta), a more complex model would need to be built, matching more of the types of circuits in the brain, possibly including structures modeled after both the hippocampus (as in [8]) and the thalamus (as in [2]). Another change that would make the simulation more realistic is using more neurons, since in the model by Abuhassan et. al. ([1]), they only used 1,000.

6 References

[1] Kamal Abuhassan, Damien Coyle, and Liam P. Maguire. "Investigating the Neural Correlates of Pathological Cortical Networks in Alzheimer's Disease Using Heterogeneous Neuronal Models". In: *IEEE Transactions on Biomedical Engineering* 59.3 (2012), pp. 890–896. DOI: https://doi.org/10.1109/TBME.2011.2181843.

[2] Basabdatta Sen Bhattacharya, Damien Coyle, and Liam P. Maguire. "A thalamo–cortico –thalamic neural mass model to study alpha rhythms in Alzheimer's disease". In: *Neural Networks* 24.6 (2011), pp. 631–645. DOI: https://doi.org/10.1016/j.neunet.2011.02.009.

[3] Viviana Culmone and Michele Migliore. “Progressive effect of beta amyloid peptides accumulation on CA1 pyramidal neurons: a model study suggesting possible treatments”. In: *Frontiers in Computational Neuroscience* 6.52 (2012). DOI: https://doi.org/10.3389/fncom.2012.00052.

[4] Eugene M. Izhikevich. “Simple Model of Spiking Neurons”. In: *IEEE Transactions on Neural Networks* 14.6 (2003), pp. 1569–1572. DOI: https://doi.org/10.1109/TNN.2003.820440.

[5] Jaeseung Jeong. “EEG dynamics in patients with Alzheimer’s disease”. In: *Clinical Neurophysiology* 115.7 (2004), pp. 1490–1505. DOI: https://doi.org/10.1016/j.clinph.2004.01.001.

[6] Peter D. Welch. “The Use of Fast Fourier Transform for the Estimation of Power Spectra: A Method Based on Time Averaging Over Short, Modified Periodogram”. In: *IEEE Transactions on Audio and Electroacoustics* AU-15.2 (1967), pp. 70–73. DOI: https://doi.org/10.1109/TAU.1967.1161901.

[7] Brendan P Zietsch et al. “Common and specific genetic influences on EEG power bands delta, theta, alpha, and beta”. In: *Biological Psychology* 75.2 (2007), pp. 154–164. DOI: https://doi.org/10.1016/j.biopsycho.2007.01.004.

[8] Xin Zou et al. “Computational Study of Hippocampal-Septal Theta Rhythm Changes Due to Beta-Amyloid-Altered Ionic Channels”. In: *PLoS ONE* 6.6 (2011), e21579. DOI: https://doi.org/10.1371/journal.pone.0021579.

7 Appendix

```python
import numpy as np
import matplotlib.pyplot as plt
from scipy import signal, stats
import pandas as pd

def run_simulation(numEx, numIn, time_max, param_a, param_b):
    totalNum = numEx + numIn

    r = stats.uniform.rvs(size=(totalNum))

    # Param a
    scale = np.ones(totalNum)
    # Param b
    uSens = np.ones(totalNum)
    # Param c
    reset = np.ones(totalNum)
    # Param d
    uReset = np.ones(totalNum)

    # Param a for excitatory neurons
    scale[0 : numEx] *= param_a
    # Param a for inhibitory neurons
    scale[numEx : ] *= 0.02 + 0.08 * r[numEx : ]

    # Param b for excitatory neurons
    uSens[0 : numEx] *= param_b
```

```
    # Param b for inhibitory neurons
    uSens[numEx : ] *= 0.25 - 0.05 * r[numEx : ]

    # Param c for excitatory neurons
    reset[0 : numEx] *= -65 + 15 * r[0 : numEx] ** 2
    # Param c for inhibitory neurons
    reset[numEx : ] *= -65

    # Param d for excitatory neurons
    uReset[0 : numEx] *= 8 - 6 * r[0 : numEx] ** 2
    # Param d for inhibitory neurons
    uReset[numEx : ] *= 2

    # Fully connected network
    synapses = np.ones((totalNum, totalNum))
    synapses[0 : numEx] *= 0.5 * stats.uniform.rvs(size=(numEx,totalNum))
    synapses[numEx : ] *= -stats.uniform.rvs(size=(numIn,totalNum))

    # Initial v for every neuron
    voltage = np.full(totalNum, -65.0)
    # Initial u for every neuron
    recovery = np.multiply( voltage,  uSens)
    # Initial thalamic input
    input = np.zeros(totalNum)

    # Run the simulation
    spikes_per_t = []
    spikes = []
    times = []
    for t in range(time_max):
        input[0 : numEx] = 5.0 * stats.norm.rvs(size=numEx)
        input[numEx : ] = 2.0 * stats.norm.rvs(size=numIn)

        pSpikes = np.where(voltage >= 30.0)[0]
        input += synapses[pSpikes, :].sum(axis=0)

        # if v >= 30 mV, v = c
        voltage[pSpikes] = reset[pSpikes]
        # if v >= 30 mV, u += d
        recovery[pSpikes] += uReset[pSpikes]

        # v += 0.04v^2 + 5v + 140 - u + I
        voltage += 0.5 * (0.04 * voltage ** 2 +
                          5.0 * voltage + 140 - recovery + input)
        voltage += 0.5 * (0.04 * voltage ** 2 +
                          5.0 * voltage + 140 - recovery + input)
        # u += a(bv - u)
        recovery += scale * (voltage * uSens - recovery)

        voltage[np.where(voltage >= 30.0)] = 30.0

        spikes_per_t.append(len(pSpikes))
        for n in pSpikes:
            spikes.append(n)
            times.append(t)

    # Obtain the last second of the simulation
    times_nparray = np.array(times)
    spikes_nparray = np.array(spikes)
    index = np.where(times_nparray >= 29000)[0][0]
    spikes_train = np.array(spikes_per_t[-1000:])

    return times_nparray[index:], spikes_nparray[index:], spikes_train

def plot_neuron_spiking(times, spikes, numEx, spikes_per_t):
    fig = plt.figure(figsize=(6,6))
    ax1 = fig.add_subplot(111)

    # Plot of spikes of each neuron over time
    ax1.plot(times, spikes, ',k')
    xl, xr = ax1.get_xlim()
    yb, yt = ax1.get_ylim()
```

```
    ax1.set_aspect(abs((xr - xl) / (yb - yt))  * 1.0)
    ax1.axhline(color='r', y=numEx - 0.5, xmax=len(spikes_per_t))
    plt.show()

    # Plot of total spikes of 1000 neurons over time
    plt.figure()
    plt.plot(range(len(spikes_per_t)), spikes_per_t)
    plt.show()

def get_power_for_each_bandwidth(numEx, numIn, time_max, param_a, param_b, Fs, trials, plot):
    total_ps = np.zeros(501)

    for i in range(trials):
        # Run simulation and return results after 29000ms
        _, _, spikes_per_t = run_simulation(numEx, numIn, time_max, param_a, param_b)
        # Get the power spectrum of the spikes
        f, Pxx_spec = signal.welch(spikes_per_t, Fs, nperseg = 1 * Fs, scaling='spectrum')
        # Sum the power spectrum
        total_ps += np.sqrt(Pxx_spec)

    total_ps /= trials

    if plot:
        boundary = 15
        plt.plot(f, total_ps)
        plt.xlim([1, boundary])
        plt.xticks(np.arange(0, boundary + 1, 1))
        plt.show()

    delta = np.sum(total_ps[1:4])
    theta = np.sum(total_ps[4:8])
    alpha = np.sum(total_ps[8:13])
    beta1 = np.sum(total_ps[13:19])
    beta2 = np.sum(total_ps[19:22])
    beta3 = np.sum(total_ps[22:31])
    gamma = np.sum(total_ps[31:51])
    full = np.sum(total_ps[1:71])

    return np.array([delta, theta, alpha, beta1, beta2, beta3, gamma, full])

# Totle simulation time
time_max = 30000     # in ms
# Frequency
Fs = 1000
# Number of trials
trials = 10

# Control group
numEx = 800
numIn = 200
param_a = 0.02
param_b = 0.2
control = get_power_for_each_bandwidth(numEx, numIn, time_max, param_a, param_b, Fs, trials, True)
control

# Decreasing number of excitatory neurons
percent_ds = np.arange(0.0075, 0.046, 0.0025)
numExs = np.array([int(800 * (1 - d)) for d in percent_ds])
numIn = 200
param_a = 0.02
param_b = 0.2
numEx_dec = []

for numEx in numExs:
    result = get_power_for_each_bandwidth(numEx, numIn, time_max, param_a, param_b, Fs, trials, True)
    numEx_dec.append(result)
```

```
numEx_dec = np.array(numEx_dec)

min_numEx_dec = np.min(numEx_dec, axis = 0)
decrease_percentage = np.zeros(len(control))
for i in range(len(control)):
    decrease_percentage[i] = 100 * (control[i] - min_numEx_dec[i]) / control[i]

case_study1 = np.array([control, min_numEx_dec, decrease_percentage])
table2 = pd.DataFrame(case_study1, columns=['delta', 'theta', 'alpha', 'beta1', 'beta2', 'beta3', 'gamma', 'full'])
table2

# Decreasing parameter b
param_bs = np.arange(0.195, 0.1996, 0.0005)
numEx = 800
numIn = 200
param_a = 0.02
param_b_dec = []

for param_b in param_bs:
    result = get_power_for_each_bandwidth(numEx, numIn, time_max, param_a, param_b, Fs, trials, True)
    param_b_dec.append(result)
param_b_dec = np.array(param_b_dec)

min_param_b_dec = np.min(param_b_dec, axis = 0)
decrease_percentage = np.zeros(len(control))
for i in range(len(control)):
    decrease_percentage[i] = 100 * (control[i] - min_param_b_dec[i]) / control[i]

case_study2 = np.array([control, min_param_b_dec, decrease_percentage])
table3 = pd.DataFrame(case_study2, columns=['delta', 'theta', 'alpha', 'beta1', 'beta2', 'beta3', 'gamma', 'full'])
table3

# Decreasing parameter a
param_as = np.arange(0.0195, 0.01996, 0.00005)
numEx = 800
numIn = 200
param_a = 0.2
param_a_dec = []

for param_a in param_as:
    result = get_power_for_each_bandwidth(numEx, numIn, time_max, param_a, param_b, Fs, trials, True)
    param_a_dec.append(result)
param_a_dec = np.array(param_a_dec)

min_param_a_dec = np.min(param_a_dec, axis = 0)
decrease_percentage = np.zeros(len(control))
for i in range(len(control)):
    decrease_percentage[i] = 100 * (control[i] - min_param_a_dec[i]) / control[i]

case_study3 = np.array([control, min_param_a_dec, decrease_percentage])
table4 = pd.DataFrame(case_study3, columns=['delta', 'theta', 'alpha', 'beta1', 'beta2', 'beta3', 'gamma', 'full'])
table4
```

Investigating the Neural Correlates of Pathological Cortical Networks in Alzheimer's Disease Using Heterogeneous Neuronal Models

Kamal Abuhassan*, Damien Coyle, *Member, IEEE*, and Liam P. Maguire

***Abstract*—This paper describes an investigation into the pathophysiological causes of abnormal cortical oscillations in Alzheimer's disease (AD) using two heterogeneous neuronal network models. The effect of excitatory circuit disruption on the beta band power (13–30 Hz) using a conductance-based network model of 200 neurons is assessed. Then, the neural correlates of abnormal cortical oscillations in different frequency bands based on a larger network model of 1000 neurons consisting of different types of cortical neurons are also analyzed. EEG studies in AD patients have shown that beta band power (13–30 Hz) decreased in the early stages of the disease with a parallel increase in theta band power (4–7 Hz). This abnormal change progresses with the later stages of the disease but with decreased power spectra in other fast frequency bands plus an increase in delta band power (1–3 Hz). Our results show that, despite the heterogeneity of the network models, the beta band power is significantly affected by excitatory neural and synaptic loss. Second, the results of modeling a functional impairment in the excitatory circuit shows that beta band power exhibits the most decrease compared with other bands. Previous biological experiments on different types of cultural excitatory neurons show that cortical neuronal death is mediated by dysfunctional ionic behavior that might specifically contribute to the pathogenesis of β-amyloid-peptide-induced neuronal death in AD. Our study also shows that beta band power was the first affected component when the modeled excitatory circuit begins to lose neurons and synapses.**

***Index Terms*—Alzheimer's disease (AD), computational models, EEG, functional deficits, structural impairment.**

I. Introduction

ALZHEIMER'S disease (AD) is the most common neurodegenerative disorder associated with progressive dementia. The clinical symptoms of AD are cognitive and intellectual deficits, and behavior dysfunction. In most instances, symptoms develop gradually or precipitously. AD constitutes approximately 70% of all dementia cases and is expected to affect 1 in 85 people worldwide by 2050 [1]. It has a significant impact on patients and caregivers, and generates substantial costs on health care providers in developed countries [2]. Clearly understanding the dynamics of neuronal networks in healthy and dysfunctional cortices is important and could aid in the development of effective diagnostic tools and prevention measures.

For the last few decades, EEG has been utilized for diagnosing dementias. EEG is a measure of the electrical activity along the scalp produced by a sufficiently large population of neurons. There is a strong correlation between cognitive deficit and the degree of the EEG abnormality. EEG spectral analysis in AD patients has shown a decrease in the mean frequency, alpha (8–12 Hz) and beta (13–30 Hz) band powers with a parallel increase in delta (1–3 Hz) and theta (4–7 Hz) band powers compared with those of healthy elderly subjects [3]. The attenuation of alpha band power is associated with an increase in lower alpha (8–10 Hz) band power and a parallel decrease in upper alpha (10–12 Hz) band power [4].

The EEG abnormalities in AD indicate functional and anatomical impairment of the cerebral cortex affected by the disease. More investigations are needed to provide insights to the underlying neurological basis of those abnormalities as well as to couple those findings with the severity of the disease. This study is targeted at investigating the relationship between AD EEG abnormalities and some neuropathological changes during AD using a conductance-based local neuronal network oscillating in beta band [5] and a simple larger network model of different types of cortical neurons that oscillates in different frequency bands [6].

The neuropathology of AD is characterized by an enormous neuronal and synaptic loss in the cerebral cortex and certain subcortical regions, and the formation of both neurofibrillary tangles (NFT) and neurotic plaques (NP) [7]. NFT are pathological tangles of hyperphosphorylated tau protein accumulated in the brains of AD patients; it is believed that the number of NFT is directly correlated with neuronal dysfunction as well as indicating the degree of dementia [8]. β-amyloid peptide (Aβ) is the main component of NP observed in the brains of patients with AD and has been suggested to contribute to the pathogenesis of neuronal degeneration [9].

A number of studies reported a deregulation of neuronal K+ channel function after exposure to Aβ peptide fragments, which led to remarkable perturbations in neuronal behavior [10]– [12]. These channels provide a negative feedback to the membrane potential of neurons. Thus, it regulates the neuronal dynamics including the timing of interspike intervals (time between

Manuscript received July 22, 2011; accepted November 27, 2011. Date of publication December 26, 2011; date of current version February 17, 2012. This work is supported by the Northern Ireland Department for Education and Learning under the Strengthening the All Island Research Base programme. *Asterisk indicates corresponding author.*

*K. Abuhassan is with the Intelligent Systems Research Centre, University of Ulster, Derry BT48 7JL, U.K. (e-mail: Abuhassan-k@email.ulster.ac.uk).

D. Coyle and L. P. Maguire are with the School of Computing and Intelligent Systems and the Intelligent Systems Research Centre, University of Ulster, Derry BT48 7JL, U.K. (e-mail: dh.coyle@ulster.ac.uk; lp.maguire@ulster.ac.uk).

Digital Object Identifier 10.1109/TBME.2011.2181843

spikes), setting the resting potential, and keeping action potentials short [13]. Therapeutic suggestions can be derived from computational models of dysfunctional neural behavior to slow down neural degeneration in AD.

The goal of this study is to elaborate and extend the findings in [14] and [15]. A recent modeling study of the hippocampal CA1 and medial septal regions has proposed that hippocampal theta band power is increased as a result of Aβ-induced reduction in A-type potassium current I_A in *e*-cells [16]. This suggests the differential vulnerability of neurons and synapses in different cortical and subcortical areas to Aβ fragments.

In this study, we examine the effects of neuronal/synaptic loss and deregulation of negative feedback to the membrane potential of cortical neurons (which mainly results from Aβ-induced dysfunctional K+ channels) on the oscillatory activity of cortical networks.

Firstly, the effect of excitatory circuit disruption on beta band power (13–30 Hz) is investigated using a local network model. Then, the investigation is extended to explore the underlying neurological sources of abnormal dynamics in different frequency bands based on a larger network model consisting of different types of cortical neurons.

The paper is outlined as follows. The network models are described in Section II. The results and analysis are provided in Section III. Finally, discussions and conclusion are presented in Sections IV and V, respectively.

II. Network Models

A. Local Neuronal Network

We simulated a conductance-based neuronal network of 200 cells containing 160 excitatory (*e*-cells) and 40 inhibitory (*i*-cells) neurons in the baseline (normal) case. The ratio of *e*- to *i*-cells is 4 (80%) to 1 (20%) motivated by the anatomy of the mammalian cortex [17]. The cells are connected all-to-all assuming that (*e–e*) synapses are weak within local networks [18]. Parameters and functional forms of the equations are adopted from [5].

Neurons were modeled by Hodgkin–Huxley dynamics; *i*-cells were of the form

$$C\left(\frac{dV_i}{dt}\right) = -g_L(V_i - V_L) - g_K n^4(V_1 - V_K) - g_{\mathrm{Na}} m^3 h(V_i - V_{\mathrm{Na}}) - I_{\mathrm{syn},i} + I_0 \quad (1)$$

and the *e*-cells were modeled by the equations

$$C\left(\frac{dV_e}{dt}\right) = -g_L(V_e - V_L) - g_K n^4(V_e - V_K) - g_{\mathrm{Na}} m^3 h(V_e - V_{\mathrm{Na}}) - g_{\mathrm{AHP}} w(V_e - V_K) - I_{\mathrm{syn},e} + I_0. \quad (2)$$

Both types of cells have a leak (*L*), transient sodium (Na), and delayed rectifier potassium (K) current. The *e*-cells have an additional after-depolarizing potential (AHP) resulting in a slow outward potassium current.

The maximal conductances were $g_{\mathrm{Na}} = 100\,\mathrm{mS/cm^2}$, $g_K = 80\,\mathrm{mS/cm^2}$, $g_L = 0.1\,\mathrm{mS/cm^2}$, and $g_{\mathrm{AHP}} = 0.3\,\mathrm{mS/cm^2}$. Reversal potentials were $V_L = -67$ mV, $V_K = -100$ mV, and $V_{\mathrm{Na}} = 50$ mV. The capacitances for *e*- and *i*-cells were 1 AF/cm^2. Parameters for both the *e*- and *i*-cells were the same; the only differences are in the synaptic currents and the driving currents, I_0. The gating variables *m*, *h*, *n* satisfy equations of the form

$$\frac{dx}{dt} = a_x(V)(1-x) - b_x(V)(x). \quad (3)$$

For $x = m, h, n$ where

$$a_m(V) = \frac{0.32(54+V)}{(1-\exp([-(V+54)/4]))} \quad (4)$$

$$b_m(V) = \frac{0.28(V+27)}{(\exp([(V+27)/5]) - 1)} \quad (5)$$

$$a_h(V) = 0.128\,\exp\left[\frac{-(V+50)}{18}\right] \quad (6)$$

$$b_h(V) = \frac{4}{(1+\exp([-(V+27)/5]))} \quad (7)$$

$$a_n(V) = \frac{0.032(V+52)}{(1-\exp([-(V+52)/5]))} \quad (8)$$

$$b_n(V) = 0.5\,\exp\left[\frac{-(57+V)}{40}\right). \quad (9)$$

The gating variable w is represented by

$$\frac{dw}{dt} = \frac{(w_\infty(V) - w)}{\tau_w(V)} \quad (10)$$

$$w_\infty(V) = \frac{1}{(1+\exp([-(V+35)/10]))} \quad (11)$$

$$\tau_w(V) = \frac{400}{(3.3\,\exp([(V+35)/20]) + \exp([-(V+35)/20]))}. \quad (12)$$

Synaptic currents were modeled as follows:

$$I_{\mathrm{syn},\alpha} = g_{i\alpha}\, s_{i,\mathrm{tot}}(V_\alpha - V_{\mathrm{in}}) + g_{e\alpha}\, s_{e,\mathrm{tot}}(V_\alpha - V_{\mathrm{ex}}) \quad (13)$$

for $\alpha = \{e, i\}$.

Reversal potentials for AMPA and GABA$_{\mathrm{A}}$ were $V_{\mathrm{ex}} = 0$ mV and $V_{\mathrm{in}} = -80$ mV, respectively. The synaptic gates satisfy:

$$s_{\alpha,\mathrm{tot}} = \frac{1}{N_\propto} \sum_{\propto-\mathrm{cells}} s_\propto \quad (14)$$

$$\frac{ds_\alpha}{dt} = a_\alpha \left(1 + \tanh\left(\frac{V_\alpha}{4}\right)\right)(1 - s_\alpha) - \left(\frac{s_\alpha}{\tau_\alpha}\right) \quad (15)$$

where $a_e = 20$/ms, $a_i = 1$/ms, $\tau_e = 2.4$ ms, and $\tau_i = 12$ ms. The inhibitory GABA$_{\mathrm{A}}$ conductances, g_{ie} and g_{ii} are 5 mS/cm^2 and 10 mS/cm^2, respectively.

The excitatory conductances were $g_{ee} = 0.01\,\mathrm{mS/cm^2}$ and $g_{ei} = 0.05\,\mathrm{mS/cm^2}$. The model time was 2000 ms and spike trains were assessed after 1000 ms allowing a settlement period of 1000 ms. Gaussian noise generated by a wiener process was

added to the voltages at each integration step. The magnitude of the noise was 0.5 mV^2/ms for the *e*-cells. The equations were integrated using Euler's method with a time step of 0.025 ms.

To achieve heterogeneity, the input currents (I_0) were varied in the range from 0.6 to 2.0 μA/cm^2 to the *e*-cells and from 1 to 1.1 μA/cm^2 to the *i*-cells. The release of neuromodulators such as Acetylcholine (ACh) in the rest state is lower than that in the active states. Low ACh increases the AHP currents (I_{AHP}). This motivates the choice of relatively strong AHP currents (I_{AHP}) [5].

1) Hypothesis Testing: Based on the local network model, we have investigated the effect of excitatory circuit disruption on the beta band (13–30 Hz) power. To achieve our aim, we have first run the model with physiological (normal) values of all parameters for 25 trials. Then, we repeated the same procedure, but with the loss rate of *e*-cells varied in the interval (6–19)%, i.e., the number of *e*-cells (N_e) varied in the interval (130–150).

The fast Fourier transform (FFT) technique has been applied on the spiking train produced by each network setup to calculate the power spectra within the beta frequency band (13–30 Hz). One-way repeated measures ANOVA has been used to analyze the significance of the difference in beta band power between the physiological (baseline) case and cases with an abnormal ratio of *e*- to *i*-cells (corresponding to the AD groups). *P* values less than 0.05 indicate a significant difference.

B. Larger Network Model

Spiking dynamics of neurons were simulated based on Izhikevich's model of spiking neurons [6], which can reproduce the firing patterns of all known types of hippocampal, cortical, and thalamic neurons. The spiking neuron can be expressed in the form of ordinary differential (16)–(18):

$$\frac{dV}{dt} = 0.04V^2 + 5V + 140 - u + I \tag{16}$$

$$\frac{du}{dt} = a(bV - u) \tag{17}$$

with the auxiliary after-spike resetting

$$\text{If } V \geq 30\,\text{mV}, \text{then } V \leftarrow c, u \leftarrow u + d \tag{18}$$

where the dimensionless variables *V* and *u* represent the membrane potential and the recovery variable of the neuron, respectively. The recovery variable *u* provides negative feedback to *V*, and it corresponds to the inactivation of Na+ ionic currents and activation of K+ ionic currents [6]. Dimensionless parameters *a*, *b*, *c*, and *d* (illustrated in Fig. 1) can be tuned to simulate the dynamics of inhibitory and excitatory neurons. Parameter *b* describes the sensitivity of the recovery variable *u* to the subthreshold fluctuations of the membrane potential *V*. Greater values of *b* couple *V* and *u* more strongly resulting in possible subthreshold oscillations and low-threshold spiking dynamics [6].

Spiking networks of 1000 neurons of different types, fully and randomly connected to each other with no plasticity, were simulated to investigate a number of hypotheses about the underlying causes of abnormal cortical oscillations in AD patients.

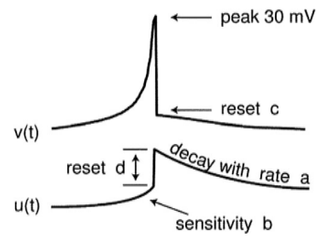

Fig. 1. Graphical representation of the influence of parameters *a*, *b*, *c*, and *d* on the spiking dynamics. (Electronic version of the figure and reproduction permissions are freely available at www.izhikevich.com.)

TABLE I
CASE STUDIES

Case study	Number of e-cells	Number of i-cells	Loss rate (%) of e-cells	Parameter b for e-cells
1	764 - 794 [a]	200	0.75% - 4.5%	0.2
2	800	200	0	0.195-0.1995 [b]

Model's setup for the investigated case studies. A number of parameters have been scaled to track the effect of changing such parameters on the EEG dynamics of the neuronal network.
[a]The loss rate of *e*-cells in case study 1 varies from 0.75% for group 1 to 4.5% for the last group. The length of step between each group in case study 1 is 0.25, i.e., the second group has 1% loss of *e*-cells. The total number of groups in case study 1 is 17 ([(794 – 764)/2] +1+ control group).
[b]Values of parameter *b* (17) for *e*-cells were decreased from 0.1995 (group 1) to 0.195 (group 10). The length of step between each group in case study 2 is 0.0005. The normal value of *b* for *e*-cells is 0.2.

The networks were stimulated by a random thalamic current at each time step. We have used MATLAB to simulate the networks in real time (resolution 1 ms). Setting the parameters of the model to physiological (normal) settings represents the physiological case. The ratio of excitatory to inhibitory neurons is 4 to 1 inspired by the anatomy of the mammalian cortex [6]. Model time was 30000 ms; spike trains were analyzed after 29000 ms allowing a settlement period (stability) of 29 s.

1) Hypothesis Testing: The model parameters are varied to test two hypotheses. The different group comparisons and associated parameter alterations have been categorized into the two case studies described in Table I. The first hypothesis is related to variations in the ratio of excitatory to inhibitory neurons in AD, while the second hypothesis is derived from AD observations of functional deficits in K+ ionic channels in cortical neurons. Each hypothesis was investigated with a computational model, as presented in Table I; each model has a different setup so that we refer to these models as case studies, i.e., hypothesis 1 was investigated in case study 1 and hypothesis 2 was investigated in case study 2.

Hypothesis 1 relies on the loss of excitatory neurons that affects the ratio of excitatory to inhibitory neurons in the cortical network and decreases the excitatory current in the network as a possible cause of abnormal network oscillations.

Hypothesis 2 links unbalanced cortical activity to an unbalanced negative feedback to the membrane potential. Specifically, it might result from dysfunctional K+ channels in excitatory neurons during AD. Hypothesis 2 suggests that the enhancement of negative feedback in excitatory neurons can be involved in abnormal oscillatory activity. This results in high-threshold spiking dynamics and less spiking activity for excitatory neurons.

To determine the overall rhythmic activity of the model in its control (normal) context, 10 trials of the model are run, each

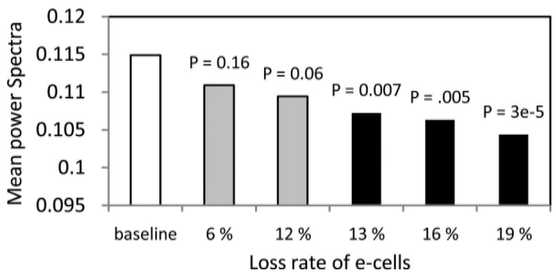

Fig. 2. Mean beta band power (13–30 Hz) for a physiological case (baseline) and cases with reduced *e*-cells. Differences (*P* values) measured by ANOVA are presented in the figure. Black bars correspond to significant differences. The number of trials is 25 for each setup.

TABLE II
MEAN POWER SPECTRA IN CASE STUDY 1

Frequency band	Min. value	Control value	Decrease percentage
Delta	3.498	3.737	6.4%
Theta	2.71	3.104	12.7%
Alpha	3.178	4.236	25%
Beta3	6.125	7.326	16.4%
Gamma	13.15	15.034	12.5%
Full	44.25	50.306	12%

Minimum and control (physiological) values of the power spectra averages for slower and faster frequency bands in case study 1. Control value is the mean power spectra of the corresponding frequency band for the control group (10 trials) with physiological values of all model's parameters.

with random input, therefore, representing 10 individuals; the healthy control group. The model parameters are then modified to test each hypothesis. Again the model is run 10 times for each test, with each test representing a group with a certain neuropathology.

The FFT tool has been applied on the spiking train produced by each model to calculate the power spectra within the following frequency bands: delta (1–3 Hz), theta (4–7 Hz), alpha (8–12 Hz), beta1 (13–18 Hz), beta2 (19–21 Hz), beta3 (22–30 Hz), gamma (30–50 Hz), and full (1–70 Hz) bands; the categorization for the frequency bands is based on [19].

One-way repeated measures ANOVA has been used to analyze statistical significance of the difference in band power within each frequency band across the different groups, as outlined previously, *P* values smaller than 0.05 were considered statistically significant.

III. RESULTS

A. Decrease in Beta Band Power Induced by Loss of Excitatory Neurons and Synapses in the Local Network Model

A significant decrease in beta band power was observed after the excitatory circuit looses more than 20 *e*-cells (number of *e*-cells becomes $\leq$139, loss rate $\geq$13%, $P < 0.05$), as illustrated in Fig. 2.

We refer to this point as a breakdown point since the power spectra of beta rhythm exhibits a significant decrease after this point. In the network model, the death of each *e*-cell is associated with a synaptic loss of 319 excitatory synapses (1% loss of excitatory synapses) since the network is fully connected (each *e*-cell receives 159 e-synapses, innervates 159 *e*-cells, and has one recurrent synapse with itself).

The same response point appears after varying the network setup as follows: settlement period is increased to 2 s and power spectra differences are assessed based on the spike trains collected after second 2 until second 4. Thus, model time is 4 s.

B. Effects of Varying the Number of Excitatory Neurons on the Oscillatory Activity of the Larger Network Model

In case study 1, the power spectrum averages of alpha and beta3 bands are significantly decreased when decreasing the number of *e*-cells (N_e) from 794 to 764 (loss% of *e*-cells is increased from 0.75% to 4.5%). It is expected that reducing N_e increases the amount of inhibition in the network and slows down the spiking activity, which explains the significant changes in the full band. From Table II, we can see that delta (slow rhythm) was not significantly affected, in contrast to the higher frequency bands.

Decrease percentage is calculated according to the following formula:

$$\text{Decrease}\% = \left(\frac{([\text{Control value}] - [\text{Minimum value}])}{[\text{Control value}]} \right) 100\%. \tag{19}$$

The minimum mean value was calculated by comparing the mean value of the power spectrum in the corresponding frequency band across all groups (each group contains 10 trials) in case study 1. We speculate that the power spectrum is shifted to lower frequencies with a parallel decrease in the coherence of fast rhythms, see Fig. 3(a). The statistical analyses show that the significant decrease started in beta3 band power ($N_e = 782$, 2.25% loss in *e*-cells).

This observation can be further explained by inspecting the minimum values of the power spectrum averages for slower and faster frequency bands, as given in Table II. The mean values of power spectrum for alpha and delta frequency band power for the groups in case study 1 are also presented in Fig. 3(b) and (c), respectively. The analyses show that the power spectrum in delta, theta, beta1, and beta2 bands was not significantly decreased.

C. Effects of Varying Parameter b for e-Cells on the Oscillatory Activity of the Larger Network Model

The datasets in case study 2 contained important information about the magnitude of mean power ranges in high frequency bands. As presented in Table III, there are higher shifts from alpha, beta1, beta2, and beta3 band powers than slower frequency bands similar to previous observations for case study 1 outlined previously. The beta2 band is the most affected one. Again, decreasing parameter *b* (17) for *e*-cells upregulates the negative feedback *u* to the membrane potential *V* (16), which results in high-threshold spiking dynamics and decreases the spiking activity of *e*-cells. This accounts for the activation of K^+ ionic currents and inactivation of Na^+ ionic currents [6].

Values of parameter *b* (17) for *e*-cells were decreased from 0.1995 (group 1) to 0.195 (group 10). The length of decreasing

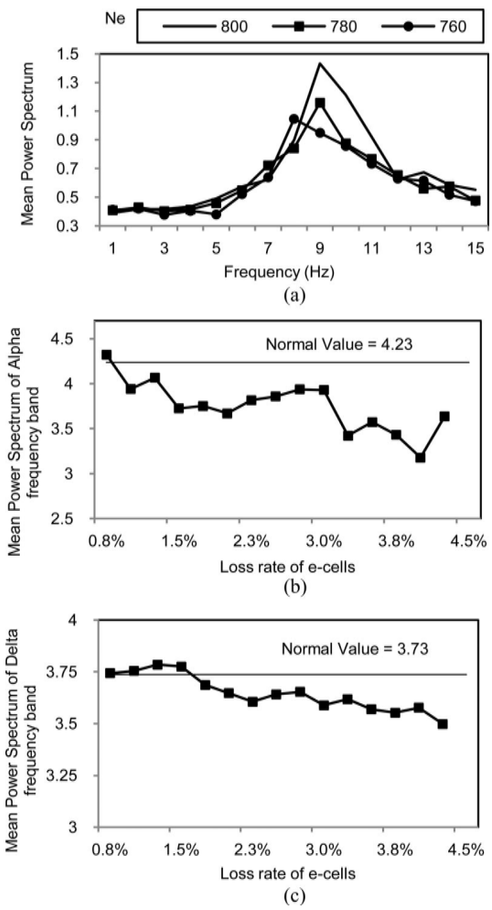

Fig. 3. Effects of increasing the loss rate of *e*-cells on the mean power spectrum. (a) Power spectrum is shifted to lower frequencies as more *e*-cells loss occurs. (b) and (c) Tracking the changes in alpha and delta band powers, respectively, as the number of *e*-cells is gradually decreased. The normal value (when $N_e = 800$ and the ratio of *e*- to *i*-cells is 4 to 1) of the mean power spectrum for delta and alpha frequency bands (control group) is indicated by a horizontal line.

step for b (17) between the groups in case study 2 is 0.0005, i.e., value of parameter b for the second group is 0.199. Control (normal) value of parameter b (17) for *e*-cells is 0.2. The total number of groups in case study 2 is 11 ($[(0.1995 - 0.195)/0.0005] + 1$ + control group). The number of trials is 10 for each setup.

In Fig. 4, we demonstrate the simulated EEG signal for three groups with different values of parameter b.

TABLE III
MEAN POWER SPECTRA AFTER VARYING PARAMETER b for *e*-CELLS (CASE STUDY 2)

Frequency band	Min. value	Control value	Decrease percentage
Delta	3.208	3.737	14.2%
Theta	2.544	3.104	18%
Alpha	2.937	4.236	30.7%
Beta1	2.671	3.579	25.4%
Beta2	1.105	1.787	38.7%
Beta3	5.359	7.326	26.9%
Gamma	11.557	15.034	23.1%
Full	39.326	50.306	21.8%

Minimum and control (physiological) values of the power spectra averages for slower and faster frequency bands in case study 2.

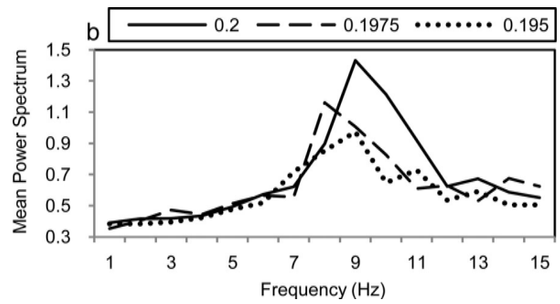

Fig. 4. Effect of decreasing parameter b for *e*-cells on the mean power spectrum.

IV. DISCUSSION

A. Structural Changes

It is commonly thought that an increase in theta band activity appears in the early stages of AD with a parallel decrease in beta activity; delta activity increases later during the course of the disease [3]. However, the underlying neural causes of abnormal EEG dynamics in AD are still poorly understood.

This research is concerned with developing a better understanding of the pathophysiological causes of abnormal cortical oscillations in AD based on a computational modeling approach.

In the current study, the effect of excitatory neural and synaptic loss on beta band power has been evaluated with two network models (along with other rhythms using the larger network model). Despite the heterogeneity of the network models, we show that the power spectrum of beta rhythm is significantly affected by excitatory neural and synaptic loss. In case study 1 (the large network model), we find that the significant decrease begins in the beta3 band (upper beta) when N_e was 782 (2.25% loss in *e*-cells).

The sequence of gradual changes in faster bands is compatible with EEG studies [3]. Although the mean power spectrum of the full band is significantly decreased, slow bands (delta and theta) are only slightly affected by the decrease and most of the signal power was shifted from fast bands toward slow bands.

The decreased activity in alpha, beta, and gamma waves is related to changes in excitatory circuit activity [20]. The study involved the analysis of a large EEG dataset using global field synchronization (GFS), a novel measure to quantify global EEG synchronization [20]. A high GFS index for a certain frequency band reflects increased functional connectivity between brain processes. The patient's results showed increased GFS values in the delta band, and decreased GFS values in alpha, beta, and gamma frequency bands, supporting the disconnection syndrome hypothesis [20] and [21].

Other AD studies have reported decreased synchronization of alpha band in the early stages of AD [22]. In a previous study [4], we utilized a classical computational model of alpha rhythm proposed by [23] to explore the relationship between synaptic activities in a thalamocortical circuitry and diminished

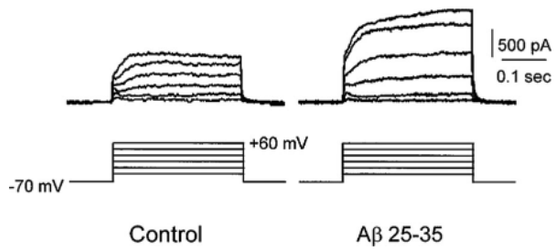

Fig. 5. Upregulation of I_K by β-amyloid 25–35 in cortical *e*-cells [24]. (Reproduced with permission from S.P. Yu.)

alpha power. In [4], it was found that the deterioration in excitatory synaptic pathways during AD biased the dynamics toward increased inhibitory activity and affected alpha rhythmic activity.

In this study, we first traced the changes in alpha band power after the structural impairments in the excitatory circuit (case study 1). We observe similar changes in alpha band power, as proposed in [4]; see Fig. 3(a). Then, we further explored the consequences of functional deficits in excitatory circuits (case study 2) on alpha band power, see Fig. 4.

According to the simulation results, we speculate that the functional deficits of ionic channels contribute to abnormal alpha band power in AD.

B. Functional Changes

It was demonstrated that cortical neuronal death is mediated by the enhancement of outward K+ current and such enhancement might specifically contribute to the pathogenesis of Aβ-induced neuronal death [24].

The results in [24] showed that Aβ fragment 1–42 or 25–35 exposure induce an upregulation in the delayed rectifier K+ current I_K, an increase in maximal conductance, and a shift in its activation voltage relationship toward hyperpolarized levels, see Fig. 5.

Cortical neuronal cultures that contained cells from different layers of cortex were used in the experiments. The cells were excitatory because they responded to N-methyl D-aspartate (NMDA) or glutamate stimulation [24].

The upregulation of this type of K+ currents provides a more negative feedback to the membrane potential of *e*-cells followed by neuronal death. We speculate that the neural mechanism that underlies the sequence of abnormal changes into EEG of AD can be described by inspecting the results in case study 2, which showed a parallel significant decrease in different bands with a higher shift from upper frequency band powers, in particular, the power spectrum of beta2 and alpha rhythms. The significant decrease within beta band power appears also (before other rhythms) when decreasing N_e, followed by a breakdown in other frequency bands when N_e decreases more and more (increased rate of neuronal and synaptic death).

V. Conclusion

The impairment of excitatory circuitry appears to play an important role in abnormal oscillatory activity of the neuronal networks and this is supported by our study, which uses simple network models. Furthermore, the observation that the death of *e*-cells is preceded by dysfunctional behavior and changes in the ionic channels has been investigated in the study. The dynamical changes of the rhythmicity in the network as a result of alterations in the negative feedback for membrane potential in *e*-cells have been focused on. Future investigations will be based on a network consisting of 100 000 cortical neurons, distribution of axonal conduction delays, long-term spike-timing-dependent synaptic plasticity, receptor kinetics, and short-term plasticity. The network structure will be informed by the organization of the cerebral cortex [25].

References

[1] R. Brookmeyer, E. Johnson, K. Ziegler-Graham, and H. M. Arrighi, "Forecasting the global burden of Alzheimer's disease," *Alzheimer's Dementia*, vol. 3, pp. 186–191, 2007.

[2] C. W. Zhu and M. Sano, "Economic considerations in the management of Alzheimer's disease," *Clin. Interventions Aging*, vol. 1, pp. 143–154, 2006.

[3] J. Jeong, "EEG dynamics in patients with Alzheimer's disease," *Clin. Neurophysiol.*, vol. 115, pp. 1490–1505, 2004.

[4] B. Sen, D. Coyle, and L. Maguire, "A thalamo–cortico–thalamic neural mass model to study alpha rhythms in Alzheimer's disease," *Neural Netw. Special Issue Brain Disorders*, vol. 24, pp. 631–645, 2011.

[5] O. Jensen, P. Goel, N. Kopell, M. Pohja, R. Hari, and B. Ermentrout, "On the human sensorimotor-cortex beta rhythm: Sources and modeling," *NeuroImage*, vol. 26, pp. 347–355, 2005.

[6] E. M. Izhikevich, "Simple model of spiking neurons," *IEEE Trans. Neural Netw.*, vol. 14, no. 6, pp. 1569–1572, Nov. 2003.

[7] D. J. Selkoe, "Alzheimer's disease is a synaptic failure," *Science*, vol. 298, pp. 789–791, 2002.

[8] J. P. Brion, "Neurofibrillary tangles and Alzheimer's disease," *Eur. Neurol.*, vol. 40, pp. 130–140, 1998.

[9] J. A. Hardy and G. A. Higgins, "Alzheimer's disease: The amyloid cascade hypothesis," *Science*, vol. 256, pp. 184–185, 1992.

[10] A. Pannaccione, F. Boscia, A. Scorziello, A. Adornetto, P. Castaldo, R. Sirabella, M. Taglialatela, G. F. Di Renzo, and L. Annunziato, "Up-regulation and increased activity of KV3.4 channels and their accessory subunit MinK-related peptide 2 induced by amyloid peptide are involved in apoptotic neuronal death," *Mol. Pharmacol.*, vol. 72, pp. 665–673, 2007.

[11] Y. Pan, X. Xu, X. Tong, and X. Wang, "Messenger RNA and protein expression analysis of voltage-gated potassium channels in the brain of Abeta(25-35)-treated rats," *J. Neurosci. Res.*, vol. 77, pp. 94–99, 2004.

[12] L. D. Plant, N. J. Webster, J. P. Boyle, M. Ramsden, D. B. Freir, C. Peers, and H. A. Pearson, "Amyloid beta peptide as a physiological modulator of neuronal 'A'-type K+ current," *Neurobiol. Aging*, vol. 27, pp. 1673–1683, 2006.

[13] S. G. Birnbaum, A. W. Varga, L.-L. Yuan, A. E. Anderson, J. D. Sweatt, and L. A. Schrader, "Structure and function of Kv4-family transient potassium channels," *Physio. Rev.*, vol. 84, pp. 803–833, 2004.

[14] K. Abuhassan, D. Coyle, and L. Maguire, "Simple spiking networks to investigate pathophysiological basis of abnormal cortical oscillations in Alzheimer's disease," *Irish J. Med. Sci.*, vol. 180, suppl. 2, pp. 62, 2011.

[15] K. Abuhassan, D. Coyle, and L. Maguire, "Employing neuronal networks to investigate the pathophysiological basis of abnormal cortical oscillations in Alzheimer's disease," in *Proc. 33rd Annu. IEEE Eng. Med. Biol. Soc. Conf.*, Boston, MA, 2011, pp. 2065–2068.

[16] X. Zou, D. Coyle, K. Wong-Lin, and L. Maguire, (2011, Jun.). Computational study of hippocampal-septal theta rhythm changes due to beta-amyloid-altered ionic channels, *PloS ONE* [Online], *6*(6). Available: http://dx.plos.org/10.1371/journal.pone.0021579.

[17] V. Braitenberg and A. Schuz, *Anatomy of the Cortex: Statistics and Geometry*. Berlin, Germany: Springer Verlag, 1991.

[18] S. R. Jones, D. J. Pinto, T. J. Kaper, and N. Kopell, "Alpha-frequency rhythms desynchronize over long cortical distances: A modeling study," *J. Comput. Neurosci*., vol. 9, pp. 271–291, 2000.
[19] Y.-M. Park, H.-J. Che, C.-H. Im, H.-T. Jung, S.-M. Bae, and S.-H. Lee, "Decreased EEG synchronization and its correlation with symptom severity in Alzheimer's disease," *Neurosci. Res*., vol. 62, pp. 112–117, 2008.
[20] T. Koenig, L. Prichep, T. Dierks, D. Hubl, L. O. Wahlund, E. R. John, and V. Jelic, "Decreased EEG synchronization in Alzheimer's disease and mild cognitive impairment," *Neurobiol. Aging*, vol. 26, pp. 165–171, 2005.
[21] X. Li, D. Coyle, L. Maguire, D. Watson, and T. McGinnity, "Grey matter concentration and effective connectivity changes in Alzheimer's disease: A longitudinal structural MRI study," *Neuroradiology*, vol. 53, pp. 733–748, 2011.
[22] J. L. Cantero, M. Atienza, A. Cruz-Vadell, A. Suarez-Gonzalez, and E. Gil-Neciga, "Increased synchronization and decreased neural complexity underlie thalamocortical oscillatory dynamics in mild cognitive impairment," *NeuroImage*, vol. 46, pp. 938–948, 2009.
[23] F. H. Lopes da Silva, A. Hoeks, H. Smits, and L. H. Zetterberg, "Model of brain rhythmic activity. The alpha-rhythm of the thalamus," *Kybernetik*, vol. 15, pp. 27–37, 1974.
[24] S. P. Yu, Z. S. Farhangrazi, H. S. Ying, C. H. Yeh, and D. W. Choi, "Enhancement of outward potassium current may participate in beta-amyloid peptide-induced cortical neuronal death," *Neurobiol. Dis*., vol. 5, pp. 81–88, 1998.
[25] E. Izhikevich, J. Gally, and G. Edelman, "Spike-timing dynamics of neuronal groups," *Cereb. Cortex*, vol. 14, pp. 933–944, 2004.

Kamal Abuhassan received a B.S. degree in computer science from Mu'tah University, Karak, Jordan, in 2002, and a M.S. degree in computer science from the University of Jordan, Amman, Jordan, in 2007. He is currently working toward the Ph.D. degree at the Intelligent Systems Research Centre, University of Ulster, Derry, U.K.

He has more than six years of experience in developing Service Oriented Architecture and J2EE applications using JAVA and IBM tools. He has been with Oracle and IBM partner companies in Jordan. He has Sun Certified Java Programmer, Sun Certified Java Web Components Developer, Sun Certified Web Services Developer, and IBM Web Content Management certifications. He is involved in developing models using MATLAB and C++ with message passing interface. His main research interests include the investigation of abnormal brain oscillation's biomarkers in Alzheimer's disease with computational modeling of neuronal networks.

Mr. Abuhassan has a research paper published in the 33rd Annual IEEE Engineering in Medicine and Biology Society Conference, Boston, MA.

Damien Coyle (M'05) received a first class degree in computing and electronic engineering and the Ph.D. degree in intelligent systems engineering from the University of Ulster, Derry, U.K., in 2002 and 2006, respectively.

Since 2006, he has been a Lecturer at the School of Computing and Intelligent Systems, University of Ulster, where he is also a member of the Intelligent Systems Research Centre. His research interests include brain-computer interfaces, computational intelligence, computational neuroscience and biomedical signal processing and he has coauthored several journal articles and book chapters in these areas.

Dr. Coyle is the 2008 recipient of the IEEE Computational Intelligence Society's (CIS) Outstanding Doctoral Dissertation Award and the 2011 recipient of the International Neural Network Society's Young Investigator of the Year Award. He received the University of Ulster's Distinguished Research Fellowship award in 2011. He coordinates the IEEE CIS Chapters activities and chairs the UKRI IEEE CIS Chapter. He is inaugural chair of the IEEE CIS Brain-Computer Interface Task Force.

Liam P. Maguire received M.Eng. and Ph.D. degrees in electrical and electronic engineering from the Queen's University, Belfast, U.K., in 1988 and 1991, respectively.

He is currently the Head of the School of Computing and Intelligent Systems, University of Ulster, Derry, U.K, where he is also the leader of the Bioinspired Systems and Neuroengineering Research Team within the Intelligent Systems Research Centre. He has an established track record of securing research funding, approximately £10M, since his appointment and has also supervised 15 Ph.D. and 3 M.Phil. students to completion. He is the author of more than 200 research papers including 70 journal papers. His research interests include fundamental research in bioinspired intelligent systems (such as the development of computational effective spiking neural networks) and the application of existing intelligent techniques in different domains.